Acceleration-Amplified Responses of Geosynthetic-Reinforced Soil Structures with a Wide Range of Input Ground Accelerations

Kuo-Hsin Yang[1] and Wen-Yi Hung[2] Erick Yusuf Kencana[3]

[1] Assistant Professor, Department of Construction Engineering, National Taiwan University of Science and Technology, No. 43 Keelung Road, Section 4, Taipei 106, Taiwan, R.O.C., Email: khy@mail.ntust.edu.tw
[2] Associate Technologist, National Center for Research on Earthquake Engineering, No. 200, Sec. 3, Xinhai Rd., Taipei 106, Taiwan, R.O.C., Email: wyhung@ncree.narl.org.tw
[3] Graduate Research Assistant, Department of Construction Engineering, National Taiwan University of Science and Technology, No. 43 Keelung Road, Section 4, Taipei 106, Taiwan, R.O.C., Email: Erick_ykLie@yahoo.com

ABSTRACT

A series of dynamic centrifuge tests is performed to investigate the acceleration-amplified and de-amplified responses within geosynthetic-reinforced soil (GRS) structures. Further, a database from various dynamic centrifuge and shaking-table tests is compiled from literature to cover a wide range of input ground accelerations in the range of 0.01–1.0g. This study demonstrates that among all factors in GRS structures (*i.e.*, structural configuration, backfill and reinforcement material, and seismic characteristics), input ground acceleration, a_g, location, z, and input motion frequency, f, have the most significant effects on acceleration-amplified responses of GRS structures. The magnitude and variation of acceleration amplification factor, A_m, which is the ratio of horizontal acceleration inside GRS structures, a_h, to input ground acceleration, a_g, decrease as a_g increases. A_m is larger than 1.0 and non-uniformly distributed with height at approximately a_g<0.40g; while A_m is less than 1.0 and generally uniformly distributed with height at a_g≥0.40g. Experimental results show that acceleration-amplified responses are highly dependent on input frequency, f. Acceleration inside GRS structures increases markedly when the predominant and fundamental frequencies are close. Further, this study examines the A_m and a_{max} relationships (*i.e.*, A_m=1.45-a_{max}/g) adopted in current GRS structure design guidelines. Comparison results indicate that the A_m and a_{max} relationship adopted in current design guidelines follows well the trend line (A_m=-0.69lna_g+0.43) regressed from complied physical data at a_g≥0.40g, but underestimates A_m at a_g<0.4g. The influence of location and frequency on A_m, as observed from physical data, is not considered in the current design guidelines.

Key Words: Acceleration amplification, Geosynthetic-reinforced structures, Dynamic centrifuge test; shaking table.

INTRODUCTION

Geosynthetic-reinforced soil (GRS) retaining structures have good proven performance against seismic loadings (*e.g.*, Tatsuoka *et al.*, 1995). Conventionally, seismic stability analyses of GRS structures are conducted within the framework of a pseudo-static approach such as the Mononobe-Okabe method. In this approach, horizontal acceleration, a_h, within GRS structures is an important parameter when evaluating seismic earth pressure. As seismic waves pass from the ground into GRS structures, amplification or attenuation of horizontal acceleration, a_h, relative to input ground acceleration, a_g, has been reported by several studies using numerical simulations (Bathurst and Hatami 1998), shaking-table tests (Huang *et al.* 2010; Krishna and Latha 2007; Matsuo *et al.* 1998) and dynamic centrifuge tests (Hung *et al.* 2011; Liu *et al*. 2010).

Current GRS structure design guidelines (*i.e.*, Elias *et al.* 2001; NCMA 2010) conventionally assume a_h is uniformly distributed with height and can be calculated using acceleration amplification factor A_m, the ratio of a_h to a_{max}, as in Eq. (1):

$$A_m=(1.45-a_{max}/g) \quad (1)$$

where A_m, a_{max}, and g are the acceleration amplification factor, maximum input acceleration, and gravity respectively. The A_m and a_{max} relationships adopted in current design guidelines were developed by Sergestin and Bastick (1988) based on finite element simulations of two steel-reinforced soil walls (6m and 10.5m high) that were subjected to ground motions in the range of 0.1–0.4g. The value of A_m is the average acceleration amplification factor along structural height. However, to the best of our knowledge, the assumed a_h distribution with height and the proposed A_m and a_{max} relationships have not been examined extensively using physical data.

In this study, a series of dynamic centrifuge tests on GRS structures is performed. Further, an experimental database from various dynamic centrifuge and shaking-table tests in literature is developed. The first objective of this study is to use compiled physical data in the database to evaluate acceleration-amplified and de-amplified responses within GRS structures, specifically for acceleration amplification factor A_m. The second objective is to examine the suitability and applicability of current seismic design methods in GRS structure design guidelines. The experimental results discussed in this study will provide insightful information and design implications for the seismic design of GRS structures.

DATABASE OF DYNAMIC GRS STRUCTURE TESTS

Centrifuge Test Program

A series of dynamic centrifuge tests was conducted at National Central University (NCU), Taiwan, to investigate the dynamic behavior of GRS embankments (Hung *et al*. 2011). All embankment models were 160 mm tall, 367mm wide at the embankment top with a facing slope of 63.5° or 45°. This embankment configuration represents an 8m-high and 18.35m-wide prototype at the target gravity level of 50g. Figure 1 shows the configuration of the centrifuge embankment model. Dry fine pure quartz sand was used as backfill in each embankment model. This pure quartz sand

was classified as poorly graded sand (SP) according to Unified Soil Classification System (USCS) with D_{50}= 0.19 mm, $\gamma_{d,max}$= 16.3 kN/m^3, $\gamma_{d,min}$=14.1 kN/m^3, and Gs=2.65. The backfill unit weight was γ=15.1 kN/m^3 and soil friction angle was ϕ=38° at the target relative density D_r=55%. Two nonwoven geotextiles were used as reinforcement in the centrifuge model. These reinforcements have ultimate tensile strength T_{ult}=1.12 and 2.24 kN/m (corresponding to T_{ult}=62.5 and 112 kN/m in prototype scale) obtained from the wide-width strip tensile test (ASTM D4595). Ten or 16 layers of reinforcement were distributed evenly inside the centrifuge model and folded backward to form a wrap-around facing. After the g level reached 50g, the base of the centrifuge models were subjected to 15 cycles of sinusoid motions for each input acceleration. Table 1 summarizes the test program, including a_g in the range of 0.01–0.23g and two different frequencies f=1 and 4.8 Hz. The embankment model was instrumented with accelerometers and linear variable differential transformers (LVDTs) to monitor acceleration inside the reinforced and retained areas and to measure model deformation respectively. Figure 2 shows one input base acceleration and acceleration measured at the top area of a GRS model. The root mean square (RMS) method was used to calculate the acceleration amplification factor, A_m, to eliminate the noisy signals possibly occurred in the acceleration records.

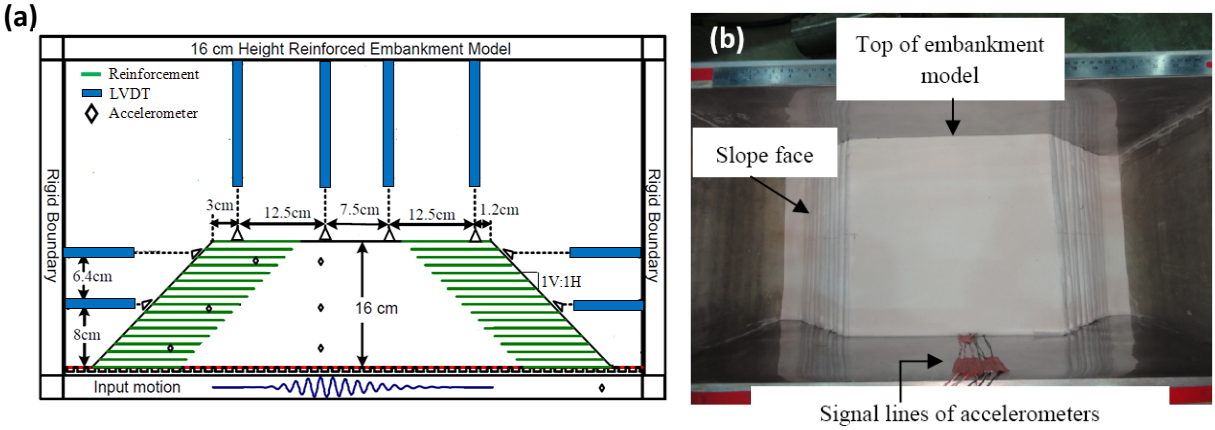

Figure 1. The centrifuge embankment model GREE8: (a) Configuration and instrumentation layouts; (b) overview

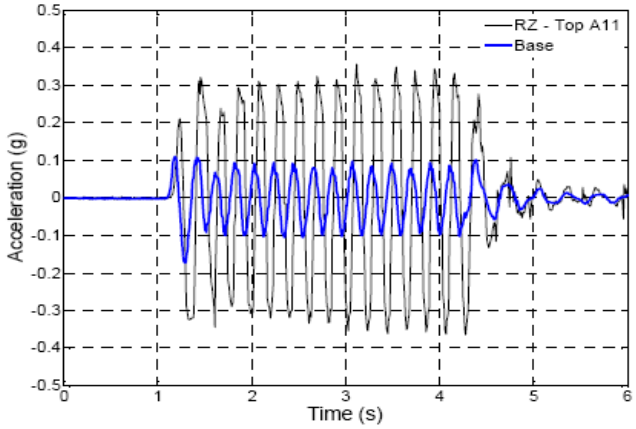

Figure 2. Input base acceleration, a_g=0.1g and f=4.8Hz, (blue line) and measured acceleration (black line) at top area of the embankment model GREE8

Table 1. Summary of centrifuge test program

Test	Vertical Spacing s_v (m)	Tensile Strength T_{ult} (kN/m)	Facing slope β (degree)	Input motion frequency f (Hz)	Input Ground Acceleration a_g (g)
GREE-4	0.8	112	45	1	0.07, 0.13, 0.22
GREE-5	0.8	112	63.5	1	0.05, 0.11, 0.20
				4.8	0.02, 0.04, 0.07
GREE-6	0.8	62.5	63.5	1	0.07, 0.13, 0.23
				4.8	0.02, 0.05, 0.10
GREE-8	0.5	112	45	1	0.04, 0.09, 0.17
				4.8	0.01, 0.03, 0.07
GREE-9	0.5	112	63.5	1	0.06, 0.11, 0.21
				4.8	0.02, 0.04, 0.10

Compilation of GRS Structure Dynamic Test Database

Other GRS structure dynamic test data collected from various dynamic centrifuge tests and shaking-table tests (Huang *et al.* 2010; Liu *et al.* 2010; Latha and Krishna 2008; Krishna and Latha 2007; Nova-Roessig and Sitar 2006; El-Eman and Bathurst 2004, 2005, 2007; Ling *et al.* 2005) were compiled into a database. Table 2 summarizes the key properties and parameters for each dynamic GRS structure test. In total, 7 series of GRS structure dynamic tests were presented. These GRS structure cases included a range of structure geometry, facing type, backfill and reinforcement material, and seismic characteristics (*e.g.,* input ground acceleration, a_g, and frequency, f). All values in Table 2 are in prototype scale.

RESULTS AND DISCUSSION

In this section, the physical data compiled in the database are used to evaluate the influence of factors on acceleration amplification factor A_m. Among all factors in Table 2 (*i.e.*, structural configuration, backfill and reinforcement material, and seismic characteristic), input ground acceleration, a_g, location, z, and input motion frequency, f, have the greatest effect on A_m. The influence of these factors on A_m is discussed as follows.

Influence of input ground acceleration on A_m

Figure 3 shows the influence of input ground acceleration, a_g, on A_m at the top area of the GRS structures where the acceleration-amplified response is greatest. The magnitude and variation of A_m decreases as a_g increases (Fig. 3). Large variation at a relatively low a_g (*i.e.*, a_g<0.2g) is likely due to the influence of other factors; particularly, seismic frequency f becomes more significant at a low a_g. The influence of input motion frequency f on A_m is discussed later. Figure 3 plots a logarithmic trend line (*i.e.*, A_m=-0.69lna_g+0.43) to depict the overall relationships between a_g and A_m. Generally, the crossover point between amplification and attenuation occurs at an a_g of about 0.40g. Strong base motion (a_g≥0.40g) results in acceleration de-amplification inside GRS structures.

Table 2. Summary of GRS structure dynamic tests

Category	Factor	Symbol (unit)	This study	Huang *et al.* (2010)	Liu *et al.* (2010)	Krishna and Latha (2007); Latha and Krishna (2008)	Nova-Roessig and Sitar (2006)	Ling *et al.* (2005)	El-Eman and Bathurst (2004, 2005, 2007)
General	Test		Dynamic centrifuge	Shaking table	Dynamic centrifuge	Shaking table	Dynamic centrifuge	Shaking table	Shaking table
	Structure type		Embankment	Slope	Wall	Wall	Embankment	Wall	Wall
Configuration	Height	H (m)	8	0.48	7.8	0.6	7.3	2.8	1
	Facing slope	β (degree)	63.4, 45	60	90	90	90, 63.4	78	90
	Facing type		Wrap-around	Aluminum plate	Aluminum block	Wrap-around	Wrap-around	Concrete block	Hollow steel
Backfill	Backfill		Fine quartz sand	Rhombically steel rod	Silty clay and sand	Local India sand	Monterey #30 sand	Fine sand	Synthetic sand
	Unit weight	γ (kN/m^3)	15	68.5	16	18	15.6, 16.2	14.3	15.7
	Initial relative density	D_r (%)	53	N/A	71	37-85	55, 75	52-56	86
	Friction angle	ϕ(degree)	35	35	23, 36	45	39.5, 42.5	38	51
	Cohesion	c(kN/m^2)	0	0	31, 0	0	0	0	0
Reinforcement	Type		Nonwoven geotextile	Nonwoven geotextile	Nonwoven geotextile	Woven geotextile	Nonwoven geotextile & wire mesh strip	Geogrid	Geogrid
	Length to height ratio	L/H	0.7	0.83	0.72	0.7	0.7, 0.9	0.6, 0.73, 0.9	0.6, 1.0
	Number of layers	n	10, 16	3	9	2, 3, 4	10, 14, 18	5, 7	4, 5
	Ultimate tensile strength	T_{ult} (kN/m)	62.5, 112	3.6	200*, 10000*	55.16	11.5, 19.7, 76.3	20, 35	12.5, 144
Seismic characteristics	Input motion		Sinusoidal	Single-cycle sinusoidal	Sinusoidal and Kobe earthquake	Sinusoidal	Sinusoidal and earthquake**	Kobe earthquake	Sinusoidal
	Method to determine Am		RMS	Maximum Value	Maximum Value	RMS	Maximum Value	Maximum Value	RMS
	Input ground acceleration	a_g (g)	0.01-0.11	0.2 - 1	0.114, 0.24	0.1, 0.15, 0.2	0.03 - 0.73	0.4, 0.8, 0.85	0.05-0.7
	Frequency	f (Hz)	1, 4.8	3, 6, 15	N/A	1, 2, 3	1.5 - 7.5	~0.35	5

*Authors only provided the information of reinforcement stiffness at 2%

** Input motions from El Centro, Loma Prieta, Santa Cruz and Kobe earthquake

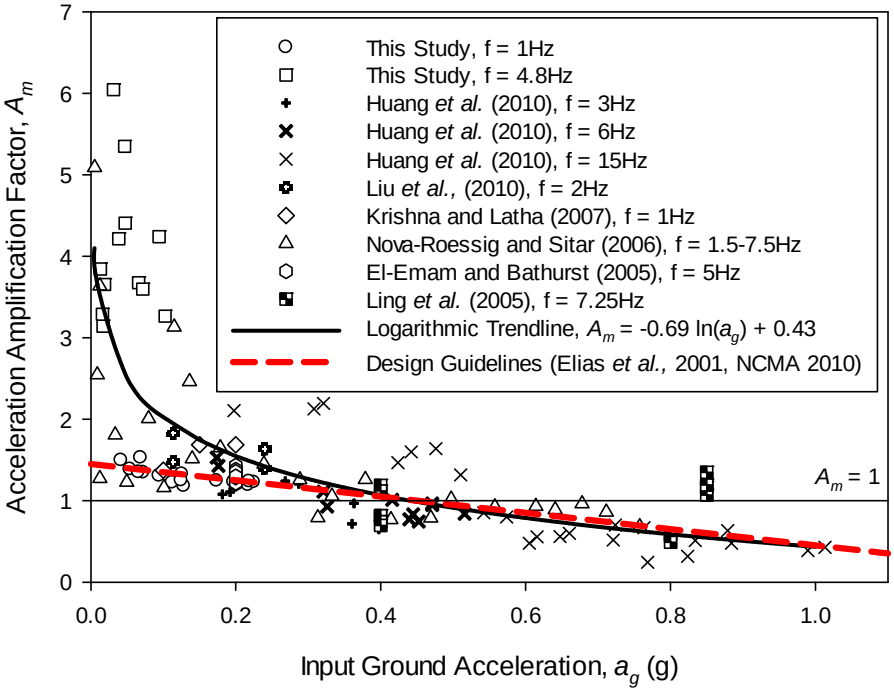

Figure 3. Influence of input ground acceleration on acceleration amplification factor at top area of GRS structures

These data are further used to examine the A_m and a_{max} relationships (*i.e.*, A_m=1.45-a_{max}/g) adopted in the two current GRS structure design guidelines (*i.e.*, Elias *et al.* 2001; NCMA 2010). The A_m and a_{max} relationships in Eq. (1) result in amplified horizontal acceleration inside GRS structures (*i.e.*, A_m>1) at a_{max}<0.45g. This result is close to the result derived using physical data (Fig. 3). Most importantly, comparison results indicate that the A_m and a_{max} relationship adopted in current design guidelines follows physical data well at $a_g \geq 0.40$g, but underestimates A_m at a_g<0.40g, and, consequently underestimate horizontal acceleration, a_h, inside GRS structures.

Influence of Location on A_m

Figure 4 shows variation of A_m with elevation inside GRS structures. The values of A_m (Fig. 4) are acquired from the trend line regressed from the database at the top, middle, and bottom areas of GRS structures separately. The distribution of A_m with height inside GRS structures is non-uniform and varies with a_g (Fig. 4) The acceleration-amplified and de-amplified responses increase as elevation increases. Acceleration amplifies (A_m>1) and the magnitude of A_m increases as elevation increases at approximately a_g<0.40g, while acceleration decreases ($A_m \leq 1$) and the magnitude of A_m decreases as elevation increases at approximately $a_g \geq 0.40$g. This observation (Fig. 4) suggests that the design of GRS structures against seismic loading should consider the change in acceleration with height. A uniform distribution of A_m with height is conventionally assumed in current design guidelines (*i.e.*, Elias *et*

al. 2001; NCMA 2010) to evaluate the seismic stability of GRS structures. However, this assumption is inconsistent with observations obtained in this study. The assumption of a uniform distribution of A_m with height may be valid at $a_g \geq 0.40$g, at which the non-uniform distribution of A_m with height is not obvious (Fig. 4). However, at $a_g < 0.40$g, the assumption of a uniform distribution may underestimate the A_m value at the top areas of GRS structures, resulting in overestimated local stability in these areas. Specifically, the effect of amplification combined with low confinement can cause local instability (*i.e.*, breakage and pullout failure) at the top few layers of reinforcements.

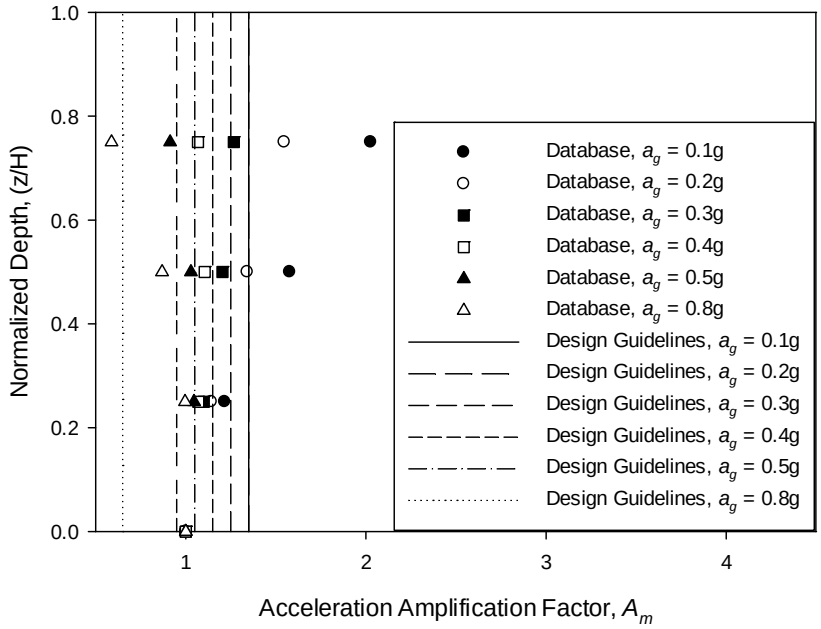

Figure 4. Influence of location on acceleration amplification factor with various input ground accelerations

Influence of Frequency on A_m

The acceleration-amplified and de-amplified responses vary significantly with acceleration frequency. This observation is demonstrated by data from this study and those from the study by Huang *et al.* (2010). Figure 5 clearly shows that A_m increases with increasing input motion frequency, f, or frequency ratio, F_r, defined as the predominant frequency of a seismic wave divided by the fundamental frequency of a structure. The fundamental frequency is $f \approx 5$–6Hz for the embankment model in this study and $f \approx 17$Hz for the GRS slope in the study by Huang *et al.* (2010).

The acceleration inside GRS structures amplifies considerably when the predominant frequency is close to the fundamental frequency (*i.e.*, F_r is close to 1.0) (Fig. 5). This is because resonance-induced oscillation as well as deformation inside GRS structures is relatively large at F_r=1.0. This observation and the above statement are supported by many research findings, including those obtained by Bathurst and

Hatami (1998) and Hatami and Bathurst (2000). Observations also show that when a wall is excited close to its fundamental frequency, the resulting displacements and reinforcement loads will be markedly greater than those of the same wall excited at the same a_g, but with a more distant predominant frequency. Clearly, acceleration response inside GRS structures is highly dependent on seismic frequency. However, the effect of frequency on A_m is not considered in current design methods such as Eq. (1). Methods incorporating the effect of frequency on A_m into Eq. (1) warrant further investigation.

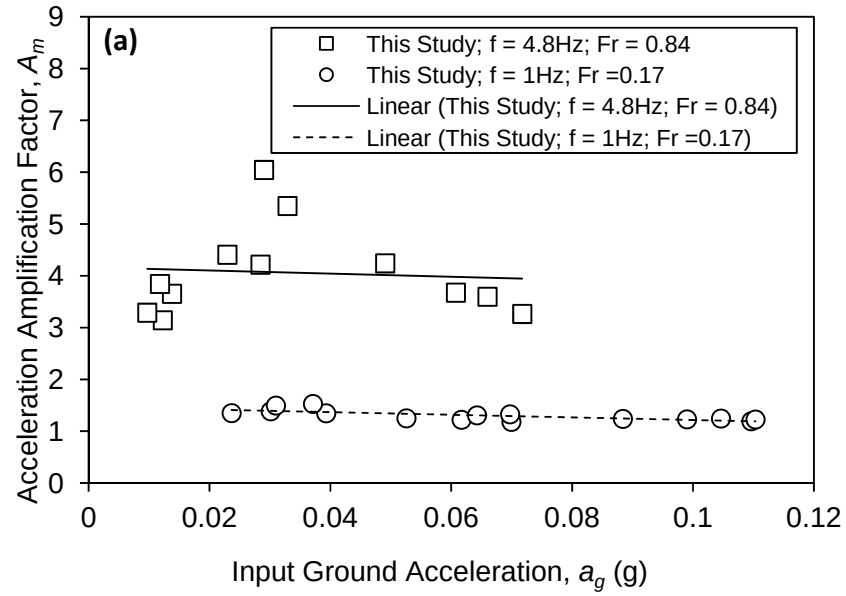

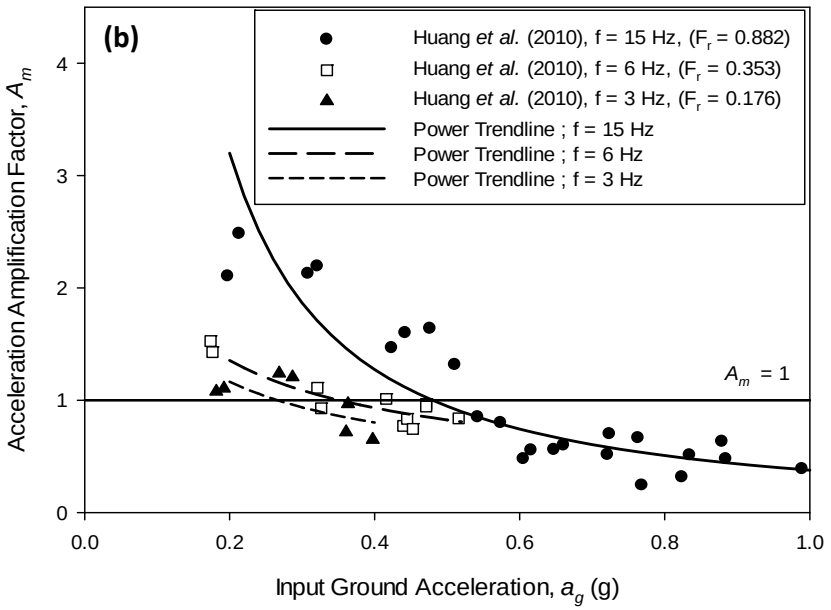

Figure 5. Influence of input motion frequency on acceleration amplification factor: (a) This study; (b) Huang *et al.* (2010)

CONCLUSIONS

In this study, physical data from various dynamic centrifuge tests and shaking-table tests on GRS structures were compiled and applied to evaluate acceleration-amplified and de-amplified responses within GRS structures, specifically for acceleration amplification factor A_m. This study shows that the acceleration amplification characteristics of GRS structures are highly dependent on input ground acceleration, a_g, location, z, and input motion frequency, f.

1. The magnitude and variation of A_m decrease as a_g increases. A large variation at a relatively low a_g (*i.e.*, $a_g \leq 0.20$g) is likely due to the influence of other factors; particularly, that of input motion frequency, f, becomes increasingly significant. Overall, horizontal acceleration inside GRS structures amplifies ($A_m > 1$) mostly at approximately $a_g < 0.40$g and de-amplifies ($A_m < 1$) at $a_g \geq 0.40$g. The A_m and a_{max} relationship adopted in current design guidelines follows physical data well at $a_g \geq 0.40$g, but underestimates A_m at $a_g < 0.40$g. This likely leads to an underestimated A_m, especially at a low a_g and, consequently, underestimates horizontal acceleration, a_h, inside GRS structures
2. The non-uniform distribution of A_m with height inside GRS structures was observed in this study. The acceleration-amplified and de-amplified responses increase as height increases. The uniform distribution of A_m with height, which is assumed in current design guidelines, may underestimate A_m at the top few layers of GRS structures when $a_g < 0.40$g, resulting in an overestimation of local stability in these areas.
3. Acceleration responses are highly dependent on seismic frequency. Thus, A_m increases as input motion frequency f increases and acceleration amplifies markedly when the predominant frequency is close to the fundamental frequency. The influence of frequency on A_m, as observed from physical data, is not considered in the current design methods.

REFERENCE

ASTM D4595. "Standard test method for tensile properties of geotextiles by the wide-width strip method." *The American Society for Testing and Materials*. West Conshohoken, PA.

Bathrust, R. J., and Hatami, K. (1998). "Seismic response analysis of a geosynthetic-reinforced soil retaining wall." *Geosynthetics International*, 5(1-2): 127-166.

El-Emam, M. and Bathrust, R.J. (2007). "Influence of reinforcement parameters on the seismic response of reduced-scale reinforced soil retaining walls." *Geotextiles and Geomembranes*, 25(1): 33 - 49.

El-Emam, M.M., and Bathurst, R.J. (2005). "Facing contribution to seismic response of reduced-scale reinforced Soil Walls." *Geosynthetic International*, 12(5): 215-238.

El-Emam, M.M., and Bathurst, R.J. (2004). "Experimental design, instrumentation and interpretation of reinforced soil wall response using a shaking table." *International Journal of Physical Modeling in Geotechnics*, 4: 13-32.

Elias, V., Christopher, B.R., and Berg, R.R. (2001). "Mechanically stabilized earth walls and reinforced soil slopes design and construction guidelines." Report

No. FHWA-NHI-00-043, *National Highway Institute, Federal Highway Administration*, Washington, D.C. March

Hatami, K., and Bathrust, R. J. (2000). "Effect of structural design on fundamental frequency of reinforced-soil retaining walls." *Soil Dynamics and Earthquake Engineering*, 19: 137-157.

Huang, C.-C., Horng, J.-C., Chueh, S.-Y., Chiou, J.-S. & Chen, C.-H. (2011). "Dynamic behavior of reinforced slopes: horizontal displacement response." *Geotextiles and Geomembranes*, 29: 257-267.

Huang, C.-C., Horng, J.-C., Chueh, S.-Y., Chiou, J.-S. & Chen, C.-H. (2010). "Dynamic behavior of reinforced slopes: horizontal acceleration response." *Geosynthetics International*, 17(4): 207-219.

Hung, W.-Y., You, T.-R., Chiou, Y,-Z., Hwang, J.-H., Lee, C.-J., Chiou, J.-S., Chen, C.-H. (2011). "Centrifuge modeling on seismic behavior of reinforced earth embedment." *Proc., The 14th Conference on Current Researches in Geotechnical Engineering in Taiwan,* August 2011

Krishna, A. M. and Latha, G.M. (2007). "Seismic response of wrap-faced reinforced soil-retaining wall models using shaking table tests." *Geosynthetics International*, 14(6): 355-364.

Latha, G., M., and Krishna, A., M., (2008). "Seismic response of reinforced soil retaining wall models: influence of backfill relative density." *Geotextile and Geomembrane*, 26: 335–349.

Ling, H. I., Mohri, Y., Leshchinsky, D., Burke, C., Matsushima, K., and Liu, H-B. (2005). "Large-scale shaking table tests on modular-block reinforced soil retaining walls." *Journal of Geotechnical and Geoenvironmental Engineering*, 131(4): 465-476.

Liu, H., Wang, X. and Song, E. (2010). "Centrifuge testing of segmental geosynthetic-reinforced soil retaining walls subject to modest seismic loading." *GeoFlorida 2010: Advance in Analysis, Modeling & Design*: 2992-2998

Matsuo, O., Tsutsumi, T., Yokoyama, K., Saito, Y. (1998). "Shaking table tests and analysis of geosynthetic-reinforced soil retaining walls." *Geosynthetics International*, 5(1-2): 97-126.

NCMA (2010). *Design manual for segmental retaining walls*, National Concrete Masonry Association Herndon, VA.

Nova-Roessig, L. and Sitar, N. (2006). "Centrifuge model studies of the seismic response of reinforced soil slopes." *Journal of Geotechnical and Geoenvironmental Engineering*, 13(3): 388-400.

Segrestin, P. and Bastick, M., J. (1988). "Seismic design of reinforced earth retaining walls - The contribution of finite elements analysis." *International Geotechnical Symposium on Theory and Practice of Earth Reinforcement*: 577-582.

Tatsuoka, F., Koseki, J. and Tateyama, M. (1995) "Performance of geogrid-reinforced soil retaining walls during the Great Hanshin-Awaji earthquake, January 17, 1995." *Proc., the First International Conference on Earthquake Geotechnical Engineering, IS Tokyo '95*: 55-62.